https://dx.doi.org/10.21577/0103-5053.20220085

J. Braz. Chem. Soc., Vol. 34, No. 1, 25-35, 2023

Article

Synthesis and Evaluation of Antibacterial Activity of 1,2,3-Triazole and Ether Derivatives of Paeonol

Laura Patricia R. Figueroa,[a] Nayara A. dos Santos,[a] Pedro Henrique O. Santiago,[b] Wanderson Romão,[a] Valdemar Lacerda Junior,[a] Javier Ellena,[b] Ana Camila Micheletti[c] and Warley S. Borges[*,a]*

[a]*Programa de Pós-Graduação em Química, Departamento de Química, Universidade Federal do Espírito Santo, 29075-910 Vitória-ES, Brazil*

[b]*Instituto de Física de São Carlos, Universidade de São Paulo, 13560-970 São Carlos-SP, Brazil*

[c]*Instituto de Química, Universidade Federal de Mato Grosso do Sul, 79070-900 Campo Grande-MS, Brazil*

Multi-drug-resistant bacteria (MDR) are the cause of different infections and diseases that have affected humanity for a long time, and have been an emerging global health problem that has led to increased morbidity and mortality. The growing emergence of MDR bacteria has underlined the need for development and discovery of new antibacterial compounds. In this context, a series of new paeonol 1,2,3-triazole and ether derivatives were synthesized using copper(I)-catalyzed azide-alkyne cycloaddition (CuAAC) reaction and nucleophilic substitution. Paeonol has been a natural product widely studied due to its many biological activities, as well as its derivatives. Three ether derivatives (two unpublished) and ten triazole derivatives (six unpublished) of paeonol were obtained, which were determined by nuclear magnetic resonance (NMR), Fourier transform infrared spectrometry (FTIR), Fourier-transform ion cyclotron resonance mass spectrometry (FT-ICR MS) and six of them by X-rays, which is the first study of this type presented for these compounds. All the synthesized compounds were evaluated as antibacterial agents against *Staphylococcus aureus* and *Escherichia coli*, obtaining a minimum inhibitory concentration (MIC) above 100 μg mL^{-1}. The results showed that CuAAC and nucleophilic substitution were very useful to obtain new paeonol triazole and ether derivatives and the products were obtained in yields from 21.3 to 98.5%. The advantages of these reactions (high yield in most compounds, reaction time, low impurities) show that using the method to produce new derivatives is advisable thus assisting in the discovery of new potential bioactive compounds.

Keywords: paeonol, triazole derivatives, ether derivatives, antibacterial

Introduction

According to recent research,[1] developing new antibacterial compounds that combat human bacterial infections is needed, due to pattern of bacterial resistance to various antimicrobial agents.

Staphylococcus aureus (*S. aureus*) is a common Gram-positive bacterium that can exist as part of the human flora[2] and can cause various clinically important infections, from superficial skin infections to deep invasive infections when it reaches the bloodstream and other organs.[3] Methicillin-resistant *S. aureus* (MRSA) and vancomycin-resistant *S. aureus* (VRSA) have also increased.[4]

Likewise, *Escherichia coli* (*E. coli*) is a Gram-negative microorganism, also considered resistant to various drugs. This microorganism can be transmitted to humans by contact with dirty surfaces and by contaminated food or water and can cause dangerous infections, leading to severe bloody diarrhea, kidney failure, or even death.[2]

Microbial infections and their associated effects are one of the biggest problems for researchers worldwide, since they represent one of the ten leading causes of mortality and the leading cause of death from microbial agents.[5] In the search for new compounds with potential antibacterial activity, many studies focus on the potential antibacterial

*e-mail: warley.borges@ufes.br
Editor handled this article: Brenno A. D. Neto (Associate)

activity of triazoles[6,7] and ethers.[8,9] Therefore, continuing to investigate their synthesis is greatly relevant.

The field of total synthesis research has been growing and gaining impetus in recent decades, due to the increased demand for potentially or biologically active rare natural products and their derivatives.[10] In the field of natural products, the starting point is a natural source where products are usually obtained in small quantities.[11] Therefore, studying synthetic methodologies and routes for the total synthesis of these bioactive natural products, sometimes more complex and in larger quantities, is important.[12]

One of the most recognized reactions used in total synthesis is the 1,3-dipolar modified Huisgen cycloaddition reaction, between a terminal alkyne (A) and an organic azide (A) catalyzed by copper (Cu^{I}), with regiospecific formation of 1,2,3-triazoles-1,4-disubstituted, being designated as "copper-catalyzed azide-alkyne cycloaddition" (CuAAC).[13] Besides, microwave irradiation considerably speeds up the CuAAC reaction, completing the reaction in minutes rather than the hours required at room temperature.

The main product of modified Huisgen cycloaddition is triazole, a five-membered cycle containing three nitrogen atoms and six pi electrons. Due to its large number of applications and diverse biological activities,[14-17] studies on this heterocyclic system have been increasing. It's origin is still synthetic, having no occurrence, therefore, in natural sources.[18]

In addition to 1,2,3-trizoles, a wide variety of compounds has drawn attention in organic synthesis research due to their different biological activities. One of these groups of compounds are the ether derivatives of natural products that are currently being studied and present excellent results.[19-23]

This study focused on derivatives of 2-hydroxy-4-methoxyacetophenone, better known as paeonol. Paeonol is the main component of one of the most used herbs in traditional medicine for over a thousand years in China, which is *Paeonia suffruticosa* (specifically the organ used in this plant is the root), the plant species belongs to the Paeoniaceae family.[24]

Paeonol is a bioactive phenol and is found in *Paeonia suffruticosa*, but also in *Dioscorea japonica*, *Arisaema erubescens* and *Paeonia lactiflora*. This compound is classified as a natural phenol and has a wide range of notable biological activities.[23] Besides, the paeonol has been used clinically as an anti-inflammatory approved by the CFDA (China Food and Drug Administration), including various dosage forms, tablet, ointment, patch and injection.[25] However, with the exception of the anti-inflammatory activity, other pharmacological activities of paeonol have not yet been clinically applied.[26]

Moreover, many paeonol derivatives with reported biological activity have been synthesized. Based on the literature, Schiff base complexes of paeonol were synthesized with Zn^{II} having high antioxidant activity,[27] with Cu^{II} having potential antioxidant activity, moderate deoxyribonucleic acid (DNA) binding activity and good cytotoxic activity of tumor cells in carcinomas of human Hep-2 cell lines[28] and paeonol with Cu^{II} and Ni^{II} being soluble in water and having DNA binding activity and high antioxidant activity.[27]

Other paeonol derivatives linked to the 1,2,3-triazole molecule were synthesized via the Huisgen-1,3-dipolar cycloaddition reaction,[29] performing the reaction with propargyl bromide and several azide commercial products and obtaining derivatives with potential antifungal activity.[30] Paeonol derivatives linked to 1,4-benzoxazinone and 1,2,3-triazole molecules with potential anticancer activity[31] and a hybrid tryptamine-triazole compound derived from paeonol were also obtained.[32]

Likewise, ether paeonol derivatives were investigated. A study synthesized a series of alkynyl ether analogues of paeonol, confirmed their structure by using infrared (IR), ^{1}H nuclear magnetic resonance (NMR), ^{13}C NMR and high-resolution mass spectrometry (HRMS), and evaluated their anti-inflammatory activity, which showed a good potential.[33] In another study, the authors[34] also made paeonol alkynyl ether analogues, and evaluated their anti-inflammatory activity, which found that two of these compounds are potent anti-inflammatories.

Therefore, this study aims to obtain compounds derived from triazoles and ethers of paeonol with possible antimicrobial activity using the Huisgen-1,3-dipolar cycloaddition reaction and nucleophilic substitution.

Experimental

General experimental procedures

Solvents with analytical grades with purity higher than 99.5% were purchase from Synth (São Paulo, SP, Brazil). Dimethylformamide, commercial azides, potassium carbonate, sodium ascorbate, copper sulfate, propargyl bromide solution (80 wt.% in toluene) and deuterated solvents were purchase from Sigma-Aldrich (St. Louis, MO, USA) and used as received. Microwave reactions were performed using a CEM Discover Synthesis Unit (CEM Corp., Matthews, USA). The machine consists of a continuous focused microwave power delivery system with operator-selectable power output from 0 to 300 W. Reactions were performed in glass vessels (capacity 10 mL) sealed with a septum. For the open layer chromatography, 5 × 30 cm and 5 × 28 cm glass columns reached with silica

gel stationary phase with a particle size of 0.04-0.063 mm and 25-40 μm packed in hexane were used.

NMR spectra were recovered on a Varian 400 MHz instrument (Palo Alto, USA) using deuterated chloroform ($CDCl_3$) as solvent and tetramethylsilane (TMS) as the internal standard both from Sigma-Aldrich (St. Louis, MO, USA). The chemical shift (δ) is in ppm and *J* values in hertz (Hz). The Fourier-transform ion cyclotron resonance mass spectrometry (FT-ICR MS) analyses were performed with a SOLARIX 9.4T mass spectrometer (Bruker Daltonics, Bremen, Germany) coupled to an electrospray source (ESI) configured to operate in positive ionization mode (ESI+); the compound dissolved in methanol (MeOH) from Sigma-Aldrich (St. Louis, MO, USA) was injected directly. This provided an unambiguous molecular formula assignment for singly charged molecular ions, such as $[M - H]^-$ or $[M + H]^+$ values. Infrared spectrum was recorded on an Agilent Technologies equipment, model Cary 630 FTIR (FTIR spectrometer) by Agilent Technologies (Santa Clara, USA), with attenuated total reflection (ATR) module, with a spectral range from 4000 to 400 cm^{-1}, 16 scans and 4 cm^{-1} resolution. The melting points were obtained by differential scanning calorimetry (DSC) in a Thermo analyzer (MDSC Q200, TA Instruments, DE, USA) with a coupled independent cooling system, all experiments were performed under a nitrogen gas atmosphere.

Single crystal X-ray diffraction

The single crystal X-ray diffraction data collection for **1b**, **1c**, **2d**, **2f**, **2h** and **2j** were performed on a Rigaku (Tokyo, Japan) XtaLAB Mini (ROW) diffractometer with Mo Kα graphite-monochromated radiation (λ = 0.71073 Å) at room temperature (293(2) K). The unit cell parameters were obtained on all reflections using the software CrysAlisPro (CrysAlisPro, Agilent Technologies Ltd, Yarnton Oxfordshire, England, 2014). The data reduction, scaling and absorption corrections were accomplished by also using the software CrysAlisPro. The structures were solved using intrinsic phasing methods in SHELXT software[35] and refined using full-matrix least-squares method with SHELXL software.[36] The Olex2 program[37] was used for the solution and refinement of the structures. In all cases, the positions of non-hydrogen atoms were determined with the Fourier maps and refined anisotropically, whereas the hydrogen atoms were stereochemically positioned by the riding model.[36] Table 1 shows the crystal data, experimental details, and refinement results.

Table 1. X-ray data collection and refinement parameters for **1b**, **1c**, **2d**, **2f**, **2h** and **2j**

	1b	**1c**	**2d**	**2f**	**2h**	**2j**
Chemical formula	$C_{16}H_{15}O_5N$	$C_{16}H_{15}O_5N$	$C_{18}H_{16}O_3N_3Br$	$C_{19}H_{16}O_3N_3F_3$	$C_{19}H_{16}O_3N_3F_3$	$C_{19}H_{19}O_4N_3$
M / (g mol^{-1})	301.29	301.29	402.25	391.35	391.35	353.37
Crystal system	triclinic	monoclinic	triclinic	monoclinic	monoclinic	triclinic
Space group	*P-1*	$P2_1/c$	*P-1*	$P2_1$	$P2_1/n$	*P-1*
a / Å	7.0994(11)	15.122(3)	5.4247(7)	13.189(5)	9.3801(12)	5.490(3)
b / Å	9.5290(11)	3.9026(9)	11.5777(13)	5.1925(13)	18.921(2)	12.379(5)
c / Å	11.6975(16)	23.822(3)	14.0763(13)	13.828(4)	10.0922(11)	14.018(4)
α / degree	110.350(12)	90	77.112(9)	90	90	111.16(3)
β / degree	93.944(12)	89.916(15)	87.673(9)	111.98(4)	96.349(11)	93.21(4)
γ / degree	106.428(12)	90	77.969(11)	90	90	102.25(4)
V / $Å^3$	699.26(18)	1405.8(4)	842.85(18)	878.1(5)	1780.2(4)	858.9(7)
Z	2	4	2	2	4	2
Density / (g cm^{-3})	1.431	1.424	1.585	1.480	1.460	1.366
θ_{min} / degree	3.044	3.189	2.609	2.698	2.814	2.827
θ_{max} / degree	26.500	24.994	26.493	25.497	26.498	25.498
ρ / mm^{-1}	0.107	0.107	2.461	0.123	0.121	0.098
Absorption correction	multi-scan	multi-scan	empirical	multi-scan	multi-scan	multi-scan
Max./min. transmission	1.000/0.430	1.000/0.292	1.000/0.840	1.000/0.225	1.000/0.923	1.000/0.236
Measured reflections	3949	3886	5014	3052	6564	4410
Independent reflections / Rint	2889/0.0141	2299/0.0427	3481/0.0726	2749/0.0687	3693/0.0181	3150
Refined parameters	202	201	228	255	256	238
R_1	0.0503	0.0780	0.0491	0.0970	0.0488	0.0945
wR_2	0.1264	0.2024	0.1231	0.2508	0.1167	0.2111
GooF	1.031	1.035	1.092	1.035	1.032	0.924
Largest diff. peak and hole / (e $Å^{-3}$)	0.2 and –0.2	0.3 and –0.3	0.7 and –0.7	0.3 and –0.3	0.2 and –0.2	0.3 and –0.2

M: molar mass; *a-c* and α-γ: unit cell parameters; V: volume; Z: formula unit *per* unit cell; R(int): internal R-value; R_1: R-value; wR^2: R-value for F^2; GooF; goodness of fit; ρ: number of electrons *per* unit volume.

The CIF files of the compounds **1b**, **1c**, **2d**, **2f**, **2h,** and **2j** were deposited in the Cambridge Structural Database (CSD) under the CCDC codes 2149421 (**1b**), 2149421 (**1c**), 2149423 (**2d**), 2149438 (**2f**), 2149439 (**2h**) and 2149422 (**2j**).

Synthesis of paeonol ethers derivatives

Synthesis of the compounds **1a-1c**

In a 50 mL round bottom flask containing paeonol (0.151 g, 0.9 mmol) in dimethylformamide (DMF) (5 mL), under stirring and ice bath, potassium carbonate (0.187 g, 1.35 mmol) was added. The system remained for 1 h in this condition. The corresponding organic halide was added in a proportion of 1, 2 equivalent and the system was kept at room temperature under stirring for 18 h (Scheme 1). The reaction solution was concentrated under reduced pressure by a rotary evaporator, the final products were purified by column chromatography using silica gel as the stationary phase, and hexane:ethyl acetate, 6:4, v/v as mobile phase for the obtained ethers.

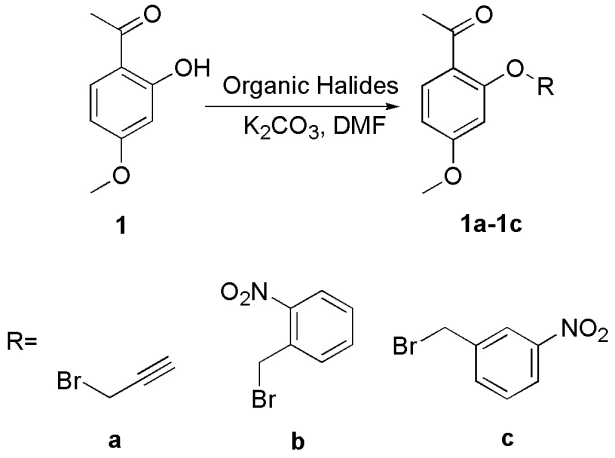

Scheme 1. General synthesis of ethers derivatives.

At the end of the process, compound **1a** (1-(4-methoxy-2-(prop-2-yn-1-yloxy)phenyl)ethan-1-one) was obtained as white solid with 95.8% yield and a melting point of 74.7 °C; thin layer chromatography (TLC): Rf = 0.77 (hexane:ethyl acetate, 7:3, v/v); FTIR (ATR) ν_{max} / cm^{-1} 3270, 3004, 2128, 1597, 1430, 1245, 1008, 961, 821; ^{1}H NMR (400 MHz, $CDCl_3$) δ 7.80 (d, 1H, *J* 9.4 Hz, CH), 6.54 (d, 1H, *J* 2.3 Hz, CH), 6.53 (dd, 1H, *J* 2.3, 9.4 Hz, CH), 4.75 (d, 2H, *J* 2.3 Hz, CH_2), 3.82 (s, 3H, CH_3), 2.57 (s, 3H, CH_3), 2.56 (t, 1H, *J* 2.3, CH); ^{13}C NMR (100 MHz, $CDCl_3$) δ 197.4 (CO), 164.1 (CO), 158.7 (CO), 132.5 (CH), 121.6 (C), 106.0 (CH), 99.6 (CH), 77.6 (CH), 76.2 (C), 56.1 (CH_2), 55.5 (CH_3), 31.8 (CH_3); ESI(+) FT-ICR MS calcd. for $C_{12}H_{13}O_3^+$ [M + H]$^+$: 205.08592; found: 205.06449; calcd. for $C_{12}H_{12}NaO_3^+$ [M + Na]$^+$: 227.06787; found: 227.06788.

Compound **1b** 1-(4-methoxy-2-((2-nitrobenzyl) oxy)phenyl)ethan-1-one was obtained as green crystals with 97.7% yield and a melting point of 110.6 °C. TLC: Rf = 0.65 (hexane:ethyl acetate, 3:2, v/v); FTIR (ATR) ν_{max} / cm^{-1} 3015, 1608, 1513, 1486, 1339, 1253, 1027, 954, 833, 733; ^{1}H NMR (400 MHz, $CDCl_3$) δ 8.17 (dd, 1H, *J* 1.3, 7.4 Hz, CH), 7.92 (dd, 1H, *J* 1.3, 7.8 Hz, CH), 7.82 (d, 1H, *J* 8.8 Hz, CH), 7.71 (td, 1H, *J* 7.8, 1.3 Hz, CH), 7.52 (td, 1H, *J* 1.3, 7.8 Hz, CH), 6.56 (dd, 1H, *J* 2.2, 8.8 Hz, CH), 6.48 (d, 1H, *J* 2.2 Hz, CH), 5.56 (s, 2H, CH_2), 3.82 (s, 3H, CH_3), 2.58 (s, 1H, CH_3); ^{13}C NMR (100 MHz, $CDCl_3$) δ 197.4 (CO), 164.3 (CO), 159.2 (CO), 147.0 (CN), 134.2 (CH), 133.0 (CH), 132.7 (C), 128.9 (CH), 128.7 (CH), 125.1 (CH), 121.4 (C), 105.6 (CH), 99.9 (CH), 67.6 (CH_2), 55.5 (CH_3), 31.4 (CH_3); ESI(+) FT-ICR MS calcd. for $C_{16}H_{16}NO_5^+$ [M + H]$^+$: 302.10230; found: 302.10205; calcd. for $C_{16}H_{15}NNaO_5^+$ [M + Na]$^+$: 324.08424; found: 324.08401; calcd. for $C_{16}H_{15}KNO_5^+$ [M + K]$^+$: 340.05818; found: 340.05797.

Compound **1c** 1-(4-methoxy-2-((3-nitrobenzyl)oxy) phenyl)ethan-1-one was obtained as yellow crystals with 73.4% yield and a melting point of 102.6 °C. TLC: Rf = 0.55 (hexane:ethyl acetate, 3:2, v/v); FTIR (ATR) ν_{max} / cm^{-1} 3087, 1605, 1524, 1438, 1345, 1253, 1021, 969, 808, 732; ^{1}H NMR (400 MHz, $CDCl_3$) δ 8.33 (brt, 1H, *J* 1.6 Hz, CH), 8.21 (ddd, 1H, *J* 1.6, 7.8 Hz, CH), 7.84 (d, 1H, *J* 8.6 Hz, CH), 7.81 (ddd, 1H, *J* 1.6, 7.8 Hz, CH), 7.60 (t, 1H, *J* 7.8 Hz, CH), 6.57 (dd, 1H, *J* 2.3, 8.6 Hz, CH), 6.49 (d, 1H, *J* 2.3 Hz, CH), 5.22 (s, 2H, CH_2), 3.83 (s, 3H, CH_3), 2.55 (s, 3H, CH_3); ^{13}C NMR (100 MHz, $CDCl_3$) δ 197.2 (CO), 164.3 (CO), 159.3 (CO), 148.4 (CN), 138.2 (C), 133.3 (CH), 133.0 (CH), 129.8 (CH), 123.2 (CH), 122.3 (CH), 121.5 (C), 105.6 (CH), 99.7 (CH), 69.4 (CH_2), 55.6 (CH_3), 31.8 (CH_3); ESI(+) FT-ICR MS calcd. for $C_{16}H_{16}NO_5^+$ [M + H]$^+$: 302.10230; found: 302.10208; calcd. for $C_{16}H_{15}NNaO_5^+$ [M + Na]$^+$: 324.08424; found: 324.08400; calcd. for $C_{16}H_{15}KNO_5^+$ [M + K]$^+$: 340.05818; found: 340.05792.

Synthesis of paeonol triazole derivatives

Synthesis of the compounds **2a-2j**

In a microwave tube (10 mL capacity) containing **1a** (1 equivalent) in 1.0 mL DMF were added 4 equivalents of azide **a-j**, 0.1 equivalents of sodium ascorbate, and 0.03 equivalents of 0.1 mol L^{-1} $CuSO_4$ solution. Subsequently, the tube was sealed, and microwave

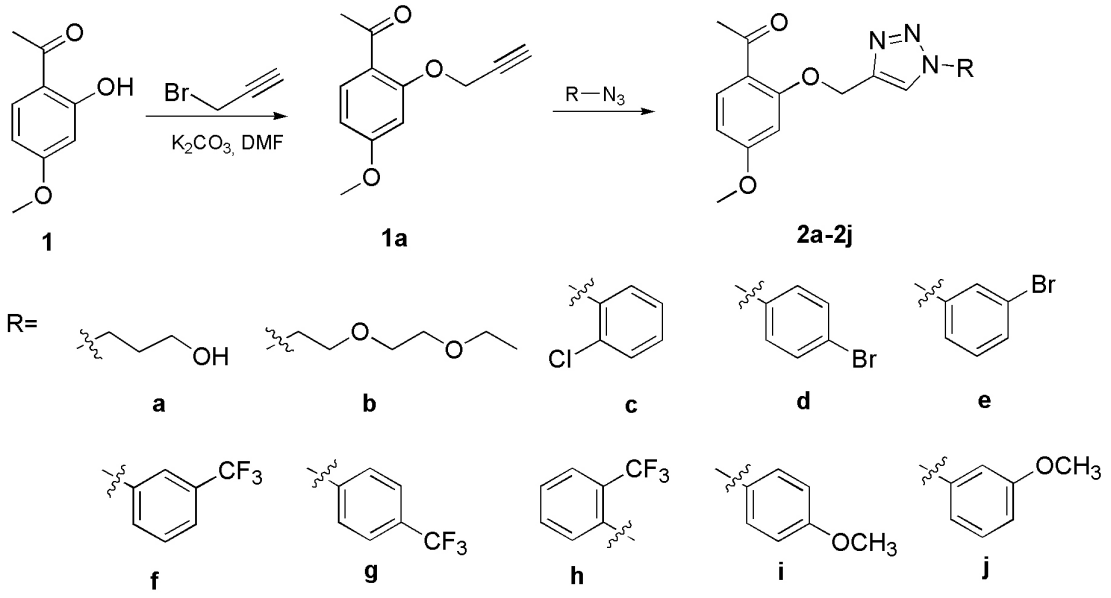

Scheme 2. General synthesis of triazole derivatives.

irradiated at 150 W, 80 °C for 5-10 min (Scheme 2). The reaction solution was concentrated under reduced pressure by a rotary evaporator, the final products were purified by column chromatography using silica gel as the stationary phase, and several mobile phases depending of each triazole obtained.

Compound **2a** 1-(2-((1-(3-hydroxypropyl)-1*H*-1,2,3-triazol-4-yl)methoxy)-4-methoxyphenyl)ethan-1-one was obtained as an orange solid with 72.3% yield and a melting point of 91.6 °C. TLC: Rf = 0.62 (ethyl acetate:methanol, 4:1, v/v); FTIR (ATR) ν_{max} / cm^{-1} 3380, 3127, 2930, 1588, 1473, 1432, 1264, 1142, 1061, 992, 830; ^{1}H NMR (400 MHz, $CDCl_3$) δ 7.77 (d, 1H, *J* 8.6 Hz, CH), 7.72 (s, 1H, CH), 6.61 (d, 1H, *J* 2.3 Hz, CH), 6.53 (dd, 1H, *J* 2.3, 8.6 Hz, CH), 5.25 (s, 2H, CH_2), 4.53 (t, 2H, *J* 6.6 Hz, CH_2), 3.83 (s, 3H, CH_3), 3.62 (t, 2H, *J* 5.9 Hz, CH_2), 2.49 (s, 3H, CH_3), 2.12 (brquint, 2H, *J* 5.9 Hz, CH_2); ^{13}C NMR (100 MHz, $CDCl_3$) δ 197.8 (CO), 164.4 (CO), 159.5 (CO), 143.1 (CN), 132.6 (CH), 123.5 (CH), 121.4 (C), 106.0 (CH), 99.5 (CH), 62.5 (CH_2), 58.5 (CH_2), 55.6 (CH_3), 47.1 (CH_2), 32.5 (CH_2), 31.7 (CH_3); ESI(+) FT-ICR MS calcd. for $C_{15}H_{20}N_3O_4^+$ $[M + H]^+$: 306.14483; found: 306.14476; calcd. for $C_{15}H_{19}N_3NaO_4^+$ $[M + Na]^+$: 328.12678; found: 328.12674; calcd. for $C_{30}H_{38}N_6NaO_8^+$ $[2M + Na]^+$: 633.26433; found: 633.26429. The final product was purified by column chromatography using silica gel as the stationary phase and ethyl acetate:hexane (7:3, v/v) as mobile phase.

Compound **2b** 1-(2-((1-(2-(2-ethoxyethoxy)ethyl)-1*H*-1,2,3-triazol-4-yl)methoxy)-4-methoxyphenyl)ethan-1-one was obtained as a yellow liquid oily with 98.5% yield. TLC: Rf = 0.3 (ethyl acetate:hexane, 7:3, v/v); FTIR (ATR) ν_{max} / cm^{-1} 3110, 2971, 1600, 1496, 1432, 1363, 1253, 1108, 1067, 964, 830; ^{1}H NMR (400 MHz, $CDCl_3$) δ 7.87 (s, 1H, CH), 7.79 (d, 1H, *J* 9.0 Hz, CH), 6.63 (d, 1H, *J* 2.3 Hz, CH), 6.52 (dd, 1H, *J* 2.3, 9.0 Hz, CH), 5.26 (s, 2H, CH_2), 4.55 (dd, 2H, *J* 5.1 Hz, CH_2), 3.85 (t, 2H, *J* 5.1 Hz, CH_2), 3.82 (s, 3H, CH_3), 3.54-3.59 (m, 2H, CH_2), 3.48-3.53 (m, 2H, CH_2), 3.46 (q, 2H, *J* 7.0 Hz, CH_2), 2.50 (s, 3H, CH_3), 1.15 (t, 3H, *J* 7.0 Hz, CH_3); ^{13}C NMR (100 MHz, $CDCl_3$) δ 197.5 (CO), 164.4 (CO), 159.6 (CO), 143.0 (CN), 132.6 (CH), 124.2 (CH), 121.3 (C), 106.0 (CH), 99.3 (CH), 70.6 (CH_2), 69.5 (CH_2), 69.3 (CH_2), 66.6 (CH_2), 62.4 (CH_2), 55.5 (CH_3), 50.5 (CH_2), 32.0 (CH_3), 15.2 (CH_3); ESI(+) FT-ICR MS calcd. for $C_{18}H_{26}N_3O_5^+$ $[M + H]^+$: 364.18670; found: 364.18668; calcd. for $C_{18}H_{25}N_3NaO_5^+$ $[M + Na]^+$: 386.16864; found: 386.16861; calcd. for $C_{36}H_{50}N_6NaO_{10}^+$ $[2M + Na]^+$: 749.34806; found: 749.34761. The final product was purified by column chromatography using silica gel as the stationary phase and hexane:ethyl acetate (3:2, v/v) as mobile phase.

Compound **2c** 1-(2-((1-(2-chlorophenyl)-1*H*-1,2,3-triazol-4-yl)methoxy)-4-methoxyphenyl)ethan-1-one was obtained as a white solid with 71.7% yield and a melting point of 121.0 °C. TLC: Rf = 0.57 (hexane:ethyl acetate, 1:1, v/v); FTIR (ATR) ν_{max} / cm^{-1} 3081, 2976, 1600, 1490, 1455, 1265, 1178, 1039, 964, 825, 755; ^{1}H NMR (400 MHz, $CDCl_3$) δ 8.10 (s, 1H, CH), 7.84 (d, 1H, *J* 8.6 Hz, CH), 7.63-7.68 (m, 1H, CH), 7.57-7.62 (m, 1H, CH), 7.44-7.51 (m, 1H, CH), 7.44-7.51 (m, 1H, CH), 6.68 (d, 1H, *J* 2.3 Hz, CH), 6.57 (dd, 1H, *J* 2.3, 8.6 Hz, CH), 5.40 (s, 2H, CH_2), 3.87 (s, 3H, CH_3), 2.56 (s, 3H, CH_3); ^{13}C NMR (100 MHz, $CDCl_3$) δ 197.5

(CO), 164.4 (CO), 159.5 (CO), 143.2 (CN), 134.7 (CCl), 132.8 (CH), 131.0 (CH), 130.8 (CH), 128.6 (CN), 128.0 (CH), 127.8 (CH), 125.0 (CH), 121.5 (C), 106.1 (CH), 99.5 (CH), 62.5 (CH_2), 55.6 (CH_3), 31.9 (CH_3); ESI (+) FT-ICR MS calcd. for $C_{18}H_{17}ClN_3O_3^+$ $[M + H]^+$: 358.09530; found: 358.09535; calcd. for $C_{18}H_{16}ClN_3NaO_3^+$ $[M + Na]^+$: 380.07724; found: 380.07725; calcd. for $C_{36}H_{32}Cl_2N_6NaO_6^+$ $[2M + Na]^+$: 737.16526; found: 737.16560. The final product was purified by column chromatography using silica gel as the stationary phase and hexane:ethyl acetate (1:1, v/v) as mobile phase.

Compound **2d** 1-(2-((1-(4-bromophenyl)-1*H*-1,2,3-triazol-4-yl)methoxy)-4-methoxyphenyl)ethan-1-one was obtained as a white crystals with 66.5% yield and a melting point of 148.3 °C. TLC: Rf = 0.67 (hexane:ethyl acetate, 1:1, v/v); FTIR (ATR) ν_{max} / cm^{-1} 3122, 2937, 1588, 1496, 1461, 1259, 1056, 1028, 970, 831, 802; ^{1}H NMR (400 MHz, $CDCl_3$) δ 8.08 (s, 1H, CH), 7.82 (d, 1H, *J* 9.0 Hz, CH), 7.66 (d, 4H, *J* 9.0 Hz, CH), 6.66 (d, 1H, *J* 2.3Hz, CH), 6.56 (dd, 1H, *J* 2.3, 9.0 Hz, CH), 5.37 (s, 2H, CH_2), 3.86 (s, 3H, CH_3), 2.56 (s, 3H, CH_3); ^{13}C NMR (100 MHz, $CDCl_3$) δ 197.5 (CO), 164.4 (CO), 159.4 (CO), 144.5 (CN), 135.8 (CN), 132.8 (CH), 133.0 (CH), 133.0 (CH), 122.7 (CBr), 122.0 (CH), 122.0 (CH), 121.5 (C), 120.8 (CH), 106.1 (CH), 99.6 (CH), 62.4 (CH_2), 55.6 (CH_3), 31.8 (CH_3); ESI(+) FT-ICR MS calcd. for $C_{18}H_{17}BrN_3O_3^+$ $[M + H]^+$: 402.04478; found: 402.04474; calcd. for $C_{18}H_{16}BrN_3NaO_3^+$ $[M + Na]^+$: 424.02673; found: 424.02671; calcd. for $C_{36}H_{32}Br_2N_6NaO_6^+$ $[2M + Na]^+$: 825.06423; found: 825.06382. The final product was purified by column chromatography using silica gel as the stationary phase and hexane:ethyl acetate (1:1, v/v) as mobile phase.

Compound **2e** 1-(2-((1-(3-bromophenyl)-1*H*-1,2,3-triazol-4-yl)methoxy)-4-methoxyphenyl)ethan-1-one was obtained as a yellow solid with 21.3% yield. TLC: Rf = 0.77 (hexane:ethyl acetate, 1:1, v/v); FTIR (ATR) ν_{max} / cm^{-1} 3116, 3018, 1588, 1490, 1432, 1259, 1044, 1015, 969, 836, 778; ^{1}H NMR (400 MHz, $CDCl_3$) δ 8.12 (s, 1H, CH), 7.95 (t, 1H, *J* 2.0 Hz, CH), 7.80 (d, 1H, *J* 9.0 Hz, CH), 7.69 (ddd, 1H, *J* 1.2, 2.0, 8.2 Hz, CH), 7.58 (ddd, 1H, *J* 1.2, 2.0, 8.2 Hz, CH), 7.40 (t, 1H, *J* 8.2 Hz, CH), 6.65 (d, 1H, *J* 2.3 Hz, CH), 6.55 (dd, 1H, *J* 2.3, 9.0 Hz, CH), 5.35 (s, 2H, CH_2), 3.85 (s, 3H, CH_3), 2.54 (s, 3H, CH_3); ^{13}C NMR (100 MHz, $CDCl_3$) δ 197.8 (CO), 164.5 (CO), 159.4 (CO), 144.3 (CN), 137.6 (CN), 132.8 (CH), 132.0 (CH), 131.1 (CH), 123.7 (CH), 123.3 (CBr), 121.3 (C), 121.1 (CH), 119.0 (CH), 106.1 (CH), 99.5 (CH), 62.2 (CH_2), 55.6 (CH_3), 31.7 (CH_3); ESI(+) FT-ICR MS calcd. for $C_{18}H_{17}BrN_3O_3^+$ $[M + H]^+$: 402.04478; found: 402.04448; calcd. for $C_{18}H_{16}BrN_3NaO_3^+$ $[M + Na]^+$: 424.02673; found: 424.02642; calcd. for $C_{18}H_{16}BrKN_3O_3^+$ $[M + K]^+$: 440.00066; found: 440.00037. The final product was purified by column chromatography using silica gel as the stationary phase and hexane:ethyl acetate (1:1, v/v) as mobile phase.

Compound **2f** 1-(4-methoxy-2-((1-(3-(trifluoromethyl) phenyl)-1*H*-1,2,3-triazol-4-yl)methoxy)phenyl)ethan-1-one was obtained as yellow crystals with 90.2% yield and a melting point of 97.6 °C. TLC: Rf = 0.46 (hexane:ethyl acetate, 3:2, v/v); FTIR (ATR) ν_{max} / cm^{-1} 3081, 2937, 1593, 1484, 1420,1264, 1120, 1033, 969, 864, 795; ^{1}H NMR (400 MHz, $CDCl_3$) δ 8.17 (s, 1H, CH), 8.05-8.07 (m, 1H, CH), 7.97 (dt, 1H, *J* 1.5, 7.6 Hz, CH), 7.83 (d, 1H, *J* 8.6 Hz, CH), 7.72-7.75 (m, 1H, CH), 7.67-7.72 (m, 1H, CH), 6.67 (d, 1H, *J* 2.3 Hz, CH), 6.57 (dd, 1H, *J* 2.3, 8.6 Hz, CH), 5.38 (s, 2H, CH_2), 3.86 (s, 3H, CH_3), 2.56 (s, 3H, CH_3); ^{13}C NMR (100 MHz, $CDCl_3$) δ 197.5 (CO), 164.4 (CO), 159.3 (CO), 144.7 (CN), 137.2 (CN), 132.7 (CF_3), 132.4 (CH), 132.9 (CH), 130.6 (CH), 125.7 (CH), 123.6 (CH), 121.5 (C), 121.0 (CH), 117.6 (CH), 106.1 (CH), 99.6 (CH), 62.3 (CH_2), 55.6 (CH_3), 31.7 (CH_3); ESI(+) FT-ICR MS calcd. for $C_{19}H_{17}F_3N_3O_3^+$ $[M + H]^+$: 392.12165; found: 392.12141; calcd. for $C_{19}H_{16}F_3N_3NaO_3^+$ $[M + Na]^+$: 414.10360; found: 414.10327; calcd. for $C_{19}H_{16}F_3KN_3O_3^+$ $[M + K]^+$: 430.07753; found: 430.07724. The final product was purified by column chromatography using silica gel as the stationary phase and hexane:ethyl acetate (3:2, v/v) as mobile phase.

Compound **2g** 1-(4-methoxy-2-((1-(4-(trifluoromethyl) phenyl)-1*H*-1,2,3-triazol-4-yl)methoxy)phenyl)ethan-1-one was obtained as a yellow solid with 91.2% yield and a melting point of 64.2 °C. TLC: Rf = 0.45 (hexane:ethyl acetate, 7:3, v/v); FTIR (ATR) ν_{max} / cm^{-1} 3116, 2983, 1594, 1444, 1426, 1248, 1109, 1028, 964, 848, 825; ^{1}H NMR (400 MHz, $CDCl_3$) δ 8.19 (s, 1H, CH), 7.90-7.94 (m, 1H, CH), 7.90-7.94 (m, 1H, CH), 7.79-7.83 (m, 1H, CH), 7.79-7.83 (m, 1H, CH), 7.82 (d, 1H, *J* 8.6 Hz, CH), 6.66 (d, 1H, *J* 2.3 Hz, CH), 6.56 (dd, 1H, *J* 2.3, 8.6 Hz, CH), 5.38 (s, 2H, CH_2), 3.86 (s, 3H, CH_3), 2.56 (s, 3H, CH_3); ^{13}C NMR (100 MHz, $CDCl_3$) δ 197.5 (CO), 164.4 (CO), 159.3 (CO), 144.7 (CN), 139.2 (CN), 132.9 (CH), 131.2 (CF_3), 130.8 (C), 127.2 (CH), 127.2 (CH), 121.4 (C), 120.9 (CH), 120.6 (CH), 120.6 (CH), 106.1 (CH), 99.6 (CH), 62.3 (CH_2), 55.6 (CH_3), 31.7 (CH_3); ESI(+) FT-ICR MS calcd. for $C_{19}H_{17}F_3N_3O_3^+$ $[M + H]^+$: 392.12165; found: 392.12166; calcd. for $C_{19}H_{16}F_3N_3NaO_3^+$ $[M + Na]^+$: 414.10360; found: 414.10357; calcd. for $C_{19}H_{16}F_3KN_3O_3^+$ $[M + K]^+$: 430.07753; found: 430.07758. The final product

was purified by column chromatography using silica gel as the stationary phase and hexane:ethyl acetate (7:3, v/v) as mobile phase.

Compound **2h** 1-(4-methoxy-2-((1-(2-(trifluoromethyl) phenyl)-1*H*-1,2,3-triazol-4-yl)methoxy)phenyl)ethan-1-one was obtained as yellow cristals with 49.5% yield and a melting point of 106.8 °C. TLC: Rf = 0.57(ethyl acetate:hexane, 3:2, v/v); FTIR (ATR) ν_{max} / cm^{-1} 3150, 2948, 1599, 1443, 1259, 1131, 1003, 963, 842, 772; ^{1}H NMR (400 MHz, $CDCl_3$) δ 7.96 (s, 1H, CH), 7.85 (brdd, 1H, *J* 1.9, 8.2 Hz, CH), 7.81 (d, 1H, *J* 8.6 Hz, CH), 7.72-7.76 (m, 1H, CH), 7.68-7.71 (m, 1H, CH), 7.57 (brd, 1H, *J* 7.4 Hz, CH), 6.64 (d, 1H, *J* 2.3 Hz, CH), 6.55 (dd, 1H, *J* 2.3, 8.6 Hz, CH), 5.36 (s, 2H, CH_2), 3.84 (s, 3H, CH_3), 2.51 (s, 3H, CH_3); ^{13}C NMR (100 MHz, $CDCl_3$) δ 197.5 (CO), 164.4 (CO), 159.5 (CO), 143.3 (CN), 133.8 (CH), 133.1 (CH), 132.9 (CN), 132.7 (CH), 131.3 (CF_3), 130.6 (CH), 128.9 (CH), 127.3 (CH), 125.7 (CH), 121.3 (CH), 106.1 (CH), 99.3 (CH), 62.2 (CH_2), 55.5 (CH_3), 31.7 (CH_3); ESI(+) FT-ICR MS calcd. for $C_{19}H_{17}F_3N_3O_3^+$ $[M + H]^+$: 392.12165; found: 392.12137; calcd. for $C_{19}H_{16}F_3N_3NaO_3^+$ $[M + Na]^+$: 414.10360; found: 414.10360; calcd. for $C_{19}H_{16}F_3KN_3O_3^+$ $[M + K]^+$: 430.07753; found: 430.07721. The final product was purified by column chromatography using silica gel as the stationary phase and ethyl acetate:hexane (3:2, v/v) as mobile phase.

Compound **2i** 1-(4-methoxy-2-((1-(4-methoxyphenyl)-1*H*-1,2,3-triazol-4-yl)methoxy)phenyl)ethan-1-one was obtained as yellow cristals with 84.5% yield and a melting point of 120.2 °C. TLC: Rf = 0.75 (ethyl acetate:hexane, 3:2, v/v); FTIR (ATR) ν_{max} / cm^{-1} 3121, 2949, 1600, 1513, 1444, 1253, 1028, 958, 825, 790; ^{1}H NMR (400 MHz, $CDCl_3$) δ 8.00 (s, 1H, CH), 7.83 (d, 1H, *J* 9.0 Hz, CH), 7.64 (d, 1H, *J* 9.0 Hz, CH), 7.64 (d, 1H, *J* 9.0 Hz, CH), 7.03 (d, 1H, *J* 9.0 Hz, CH), 7.03 (d, 1H, *J* 9.0 Hz, CH), 6.68 (d, 1H, *J* 2.3 Hz, CH), 6.56 (dd, 1H, *J* 2.3, 9.0 Hz, CH), 5.36 (s, 2H, CH_2), 3.86 (s, 3H, CH_3), 3.86 (s, 3H, CH_3), 2.56 (s, 3H, CH_3); ^{13}C NMR (100 MHz, $CDCl_3$) δ 197.5 (CO), 164.4 (CO), 160.0 (CO), 159.5 (CO), 143.9 (CN), 132.8 (CH), 130.3 (CN), 122.3 (CH), 122.3 (CH), 121.5 (C), 121.2 (CH), 114.8 (CH), 114.8 (CH), 106.1 (CH), 99.5 (CH), 62.5 (CH_2), 55.6 (CH_3), 55.6 (CH_3), 31.9 (CH_3); ESI(+) FT-ICR MS calcd. for $C_{19}H_{20}N_3O_4^+$ $[M + H]^+$: 354.14483; found: 354.82381; calcd. for $C_{19}H_{19}N_3NaO_4^+$ $[M + Na]^+$: 376.12678; found: 376.12675; calcd. for $C_{38}H_{38}N_6NaO_8^+$ $[2M + Na]^+$: 729.26433; found: 729.26444. The final product was purified by column chromatography using silica gel as the stationary phase and ethyl acetate:hexane (3:2, v/v) as mobile phase.

Compound **2j** 1-(4-methoxy-2-((1-(3-methoxyphenyl)-1*H*-1,2,3-triazol-4-yl)methoxy)phenyl)ethan-1-one was obtained as orange crystals with 71.8% yield and a melting point of 125.3 °C. TLC: Rf = 0.8 (ethyl acetate:hexane, 3:2, v/v); FTIR (ATR) ν_{max} / cm^{-1} 3115, 2924, 1599, 1501, 1426, 1264, 1044, 998, 836, 783; ^{1}H NMR (400 MHz, $CDCl_3$) δ 8.07 (s, 1H, CH), 7.83 (d, 1H, *J* 9.0 Hz, CH), 7.42 (t, 1H, *J* 8.2 Hz, CH), 7.36 (brt, 1H, *J* 2.3 Hz, CH), 7.26 (ddd, 1H, *J* 0.8, 2.3, 8.2 Hz, CH), 6.99 (ddd, 1H, *J* 0.8, 1.9, 8.2 Hz, CH), 6.68 (d, 1H, *J* 2.3 Hz, CH), 6.56 (dd, 1H, *J* 2.3, 9.0 Hz, CH), 5.37 (s, 2H, CH_2), 3.88 (s, 3H, CH_3), 3.86 (s, 3H, CH_3), 2.56 (s, 3H, CH_3); ^{13}C NMR (100 MHz, $CDCl_3$) δ 197.5 (CO), 164.4 (CO), 160.7 (CO), 159.5 (CO), 144.0 (CN), 137.8 (CN), 132.8 (CH), 130.6 (CH), 121.5 (C), 121.1 (CH), 114.9 (CH), 112.4 (CH), 106.5 (CH), 106.1 (CH), 99.5 (CH), 62.4 (CH_2), 55.6 (CH_3), 55.7 (CH_3), 31.9 (CH_3); ESI(+) FT-ICR MS calcd. for $C_{19}H_{20}N_3O_4^+$ $[M + H]^+$: 354.14483; found: 354.14491; calcd. for $C_{19}H_{19}N_3NaO_4^+$ $[M + Na]^+$: 376.12678; found: 376.12678; calcd. for $C_{38}H_{38}N_6NaO_8^+$ $[2M + Na]^+$: 729.26433; found: 729.26449. The final product was purified by column chromatography using silica gel as the stationary phase and ethyl acetate:hexane (3:2, v/v) as mobile phase.

Antibacterial activity

Round bottom 96 well plates were prepared by dispensing 100 µL of Mueller-Hinton broth (Kasvi, São José dos Pinhais, PR, Brazil) into each well. Stock solutions of each compound were prepared and serial 1:2 dilutions were performed to reach final concentrations within the 7.8-1000 µg mL^{-1} range, with a 100 µL final volume in each well. For gentamicin (Sigma-Aldrich, Saint Louis, MO, USA), used as positive control, final concentrations ranged from 60 to 0.5 µg mL^{-1}. Two standard bacterial strains were used: *Staphylococcus aureus* (NEWP0023) and *Escherichia coli* (NEWP0022), purchased from Newprov (Pinhais, PR, Brazil). The bacterial inoculum was an overnight culture grown in Mueller-Hinton agar (Sigma-Aldrich, Saint Louis, MO, USA) suspended in sterile saline solution (0.45%) at a concentration of approximately 10^8 colony forming units (CFU) mL^{-1} (0.5 in McFarland scale), measured in a MS Tecnopon (Piracicaba, SP, Brazil) MCF-500 McFarland turbidimeter. This solution was diluted 1:10 in saline solution (0.45%), and a 5 µL aliquot was added to each well. All experiments were performed in triplicate and the microdilution trays were incubated at 36 °C for 24 h. An aqueous solution (0.5%) of triphenyltetrazolium chloride (TTC, Merck, Darmstadt, Germany) was subsequently added to each well (20 µL) and the trays were incubated at 36 °C for 2 h. In the wells where

bacterial growth did occur, TTC changed from colorless to red. Minimal inhibitory concentration (MIC, expressed in μg mL^{-1}) was defined as the lowest concentration of each substance at which no color change occurred.

Results and Discussion

We used paeonol as a starting material for bimolecular nucleophilic substitution as a methodological strategy to provide three (**1a-1c**) ether compounds and the **1a** compound, alquinil paeonol, as a starting material for the 1,3-dipolar modified Huisgen cycloaddition reaction as a methodological strategy to supply ten (**2a-2j**) triazole derivatives. Their chemical structures were determined by spectrometric and spectroscopic methods such as uni and bi-dimensional ^{1}H, ^{13}C NMR, heteronuclear single quantum coherence (HSQC), heteronuclear multiple bond correlation (HMBC), high resolution electrospray ionization mass spectrometry (HR-ESI-MS) and Fourier-transform infrared spectroscopy (FTIR). Also, we determined the crystal structure of six compounds by X-ray. For all compounds, the signals observed in the NMR spectra (δ in ppm) related to the paeonol moiety were very similar, and the paeonol was compared with the literature.[38]

To obtain compound **1a**, we used an excess of potassium carbonate as a base to remove the acid hydrogen from the phenolic group in the molecule. Due to the negative charge stabilization capacity of the oxygen atom, coupled with the resonance effect, the phenoxide ion is formed and stabilized *in situ*, and then occurs the nucleophile attack on the propargyl bromide electron deficient carbon atom via bimolecular nucleophilic substitution. We observed, besides the paeonol NMR signals, a hydrogen at δ 2.56 ppm (t, *J* 2.3 Hz, 1H) coupling with a signal at δ 4.75 ppm (d, 2H, *J* 2.3 Hz) that was assigned to terminal acetylenic group. The HMBC correlation between the hydrogen with chemical shift δ 4.75 (d, 2H, *J* 2.3 Hz, CH_2) and carbon δ 55.5 (CH_3) confirmed the acetylenic group.

To form compounds **1b** and **1c**, we used the same reaction conditions described before, using 2-nitrobenzyl bromide and 3-nitrobenzyl bromide, respectively, for the bimolecular nucleophilic substitution reaction. The information obtained by uni and bi-dimensional NMR confirmed the presence of the nitro group in the *ortho* position for compound **1b** and in *meta* in compound **1c**.

The other synthetic step consisted of forming the 1,2,3-triazole ring (compounds **2a-2j**) catalyzed by Cu^{I} from **1a**. Due to their physicochemical properties such as high chemical stability, aromaticity, ability to form hydrogen bonds, and a high dipole moment these heterocycles are recommended as possible pharmacological compounds.[39] To obtain the Cu^{I} catalyst, *in situ*, copper sulfate was used as precursor, which is reduced upon contact with sodium ascorbate in weakly basic medium and released into the medium, participating in the catalytic cycle.[30]

For **2a,** the ^{1}H NMR showed two triplets and one multiplet hydrogens at δ 3.62 (t, *J* 5.8 Hz), δ 4.53 (t, *J* 6.8 Hz) and δ 2.08-2.16 (m) confirming the 1-propanol chain. The HMBC correlation of these hydrogens with carbons at δ 58.6 (CH_2), 47.2 (CH_2), and 32.6 (CH_2) confirmed the 1-propanol chain. Also, one singlet hydrogen at δ 7.71 (s) confirmed the triazole ring.

For **2b**, the ^{1}H NMR showed two triplets and two multiplets hydrogens at δ 3.85 (t, *J* 5.1 Hz), δ 1.15 (t, *J* 7.0 Hz), δ 3.54-3.59 (m) and δ 3.48-3.53 (m) and one additional double doublet and one quartet at δ 4.55 (dd, *J* 4.55, 5.5 Hz) and δ 3.46 (q, *J* 7.0 Hz) confirming the 2-(2-ethoxyethoxy)ethylethan chain. Also, one singlet hydrogen at δ 7.86 (s) confirmed the triazole ring.

Compounds **2c-2e** follows similar substitution patterns of the aromatic ring. The ^{1}H NMR spectrum shows four signals for aromatic hydrogens with different multiplicities. All three compounds showed the singlet hydrogen at δ 8.10 (s), 8.08 (s) and 8.12 (s), respectively, characteristic of the triazole ring.

Compounds **2f-2h** follow similar substitution pattern of the aromatic ring. The ^{1}H NMR spectrum shows four signals for aromatic hydrogens with different multiplicities. We confirmed the presence of the trifluoromethyl group with the ^{13}C NMR spectra showing the signal related to the trifluoromethyl group at δ 132.9, 131.3 and 131.5 ppm. All compounds showed the singlet hydrogen at δ 8.17 (s), δ 8.18 (s) and δ 7.96 (s) characteristic of the triazole ring.

Compounds **2i-2j** follows similar substitution patterns of the aromatic ring. The ^{1}H NMR spectrum showed four signals for aromatic hydrogens with different multiplicities. We observed the presence of a methoxy group in the molecules at δ 3.86 (s, 3H) and δ 55.8 ppm and at δ 3.88 (s, 3H) and δ 55.8 ppm. Both compounds showed the singlet hydrogen at δ 8.00 (s) and 8.07 (s) characteristic of the triazole ring.

The crystal structures of **1b, 1c**, **2d**, **2f**, **2h,** and **2j** were elucidated by single crystal X-ray diffraction analysis, with Figures 1 and 2 showing the ORTEP type illustrations. The X-ray data for these compounds agree with the results obtained with spectroscopic analysis.

The molecular structures of **1b** and **1c** isomers comprise a paeonol group attached to an *o*-nitrobenzyl or a *m*-nitrobenzyl group, respectively, as verified previously. In the solid state, the structure **1b** is almost planar, while the molecule of **1c** is slightly twisted, with a dihedral angle of 36.75º between the two aromatic rings. The structure of

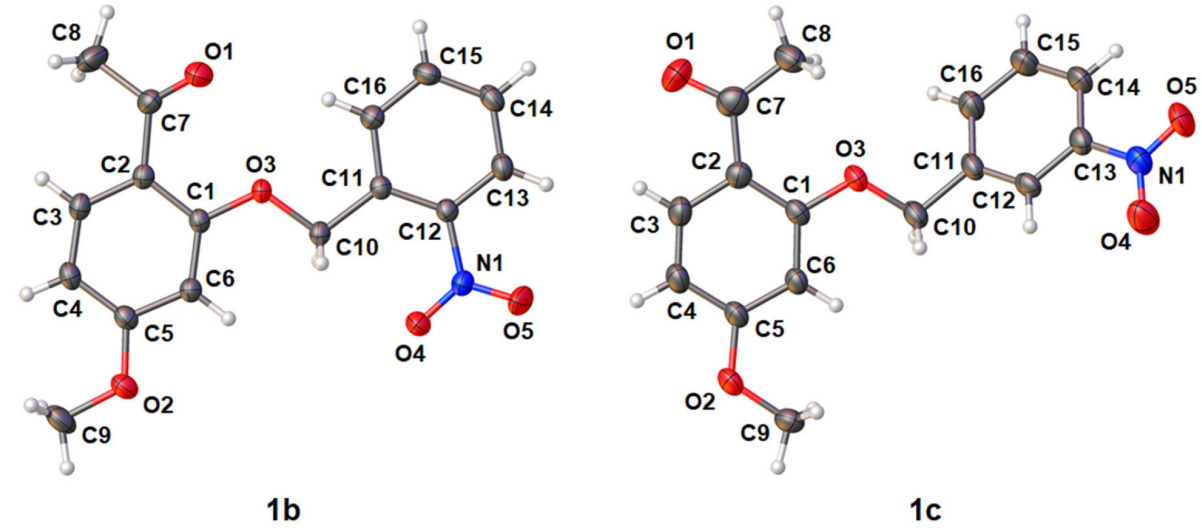

Figure 1. ORTEP type diagrams of **1b** and **1c**, showing ellipsoids at the 30% probability.

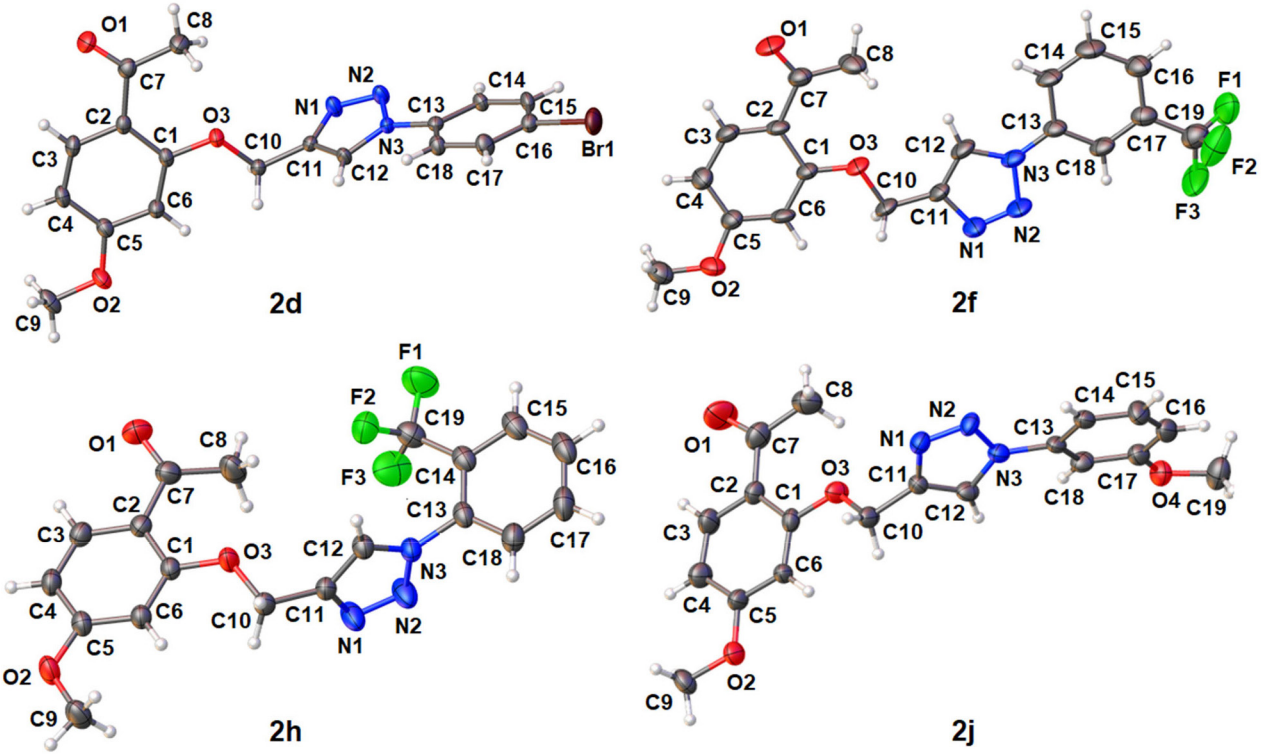

Figure 2. ORTEP type diagrams of **2d**, **2f**, **2h** and **2j**, showing ellipsoids at the 30% probability.

1b (Figure S21, Supplementary Information (SI) section) has π···π interactions between the aromatic rings stabilizing its crystal lattice and enabling the formation of a one-dimensional network. For **1c**, the C–H...O intermolecular interactions between an aromatic hydrogen atom and the acetyl group of the paeonol part stabilize the crystal forming columns along the crystallographic *b* axis (Figure S30, SI section).

We also verified the formation of the triazole ring in **2d**, **2f**, **2h** and **2j** with the X-ray data, where the $–CF_3$ group showed as *meta* and *ortho* substituent in **2f** and **2h**, respectively, whereas the bromide and the methoxy groups are in *para* and *meta* positions in **2d** and **2j**, respectively. The triazole derivatives are non-planar, with the dihedral angles between the aromatic and triazole rings ranging from 9.35 to 89.13º, except for **2f** which is almost planar and has dihedral angles lower than 6.19º. The 3-dimensional arrangements of **2d** and **2j** are stabilized by two C–H...N intermolecular interaction involving the triazole ring which form infinite chains along *a* axis (Figures S60 and S108,

SI section). Meanwhile, C–H...O interactions involving the acetyl group of the paeonol part form columns along the (010) direction in **2f** (Figure S76, SI section). Finally, we observed that C–H..O, C–H...F and C–H...N intermolecular interactions form a compact 3-dimensional packing in **2h** (Figure S92, SI section).

Biological activity

The antimicrobial activity of compounds **1** (paenol) to **2j** was evaluated by microdilution assay over a Gram-positive (*S. aureus*) and a Gram-negative (*E. coli*) standard bacterial strains. Table 2 shows the results, expressed in minimal inhibitory concentration (MIC).

Table 2 shows that none of the compounds showed antibacterial activity against the evaluated strains, since all MIC values are above 100 μg mL^{-1}.[40]

Table 2. Minimal inhibitory concentration values (MIC) for compounds **1** to **2j**

Compound	MIC / (μg mL^{-1})	
	S. aureus (NEWP0023)	*E. coli* (NEWP0022)
1	≥ 500	≥ 250
1a	≥ 500	≥ 250
1b	≥ 500	≥ 250
1c	≥ 500	≥ 250
2a	≥ 500	≥ 250
2b	≥ 500	≥ 250
2c	≥ 500	≥ 250
2d	≥ 500	≥ 250
2e	≥ 500	≥ 250
2f	250	≥ 250
2g	≥ 500	≥ 250
2h	≥ 500	≥ 250
2i	≥ 500	≥ 250
2j	≥ 500	≥ 250
Gentamicin	≤ 0.5	≤ 0.5

Conclusions

The results showed that CuAAC and nucleophilic substitution were very useful to obtain new paeonol triazole and ether derivatives, respectively. The products were obtained in high yields, from 21.3 to 98.5% and low reaction time. Structure features and functional groups of the compounds obtained indicate possible biological activity, and this is the reason why, evaluating them for their biological potential is important. This study assessed their antibacterial activity obtaining a minimum inhibitory concentration (MIC) above 100 μg mL^{-1}. The advantages of the reactions carried out show that the method is recommended for the production of new derivatives and can help in the discovery of new bioactive compounds.

Supplementary Information

Crystallographic data (excluding structure factors) for the structures in this study (**1b**, **1c**, **2d**, **2f**, **2h** and **2j**) were deposited in the Cambridge Crystallographic Data Centre as supplementary publication number CCDC2149421 (**1b**), 2149421 (**1c**), 2149423 (**2d**), 2149438 (**2f**), 2149439 (**2h**) and 2149422 (**2j**). Copies of the data can be obtained, free of charge, via https://www.ccdc.cam.ac.uk/structures/.

Supplementary information (NMR, MS, IR and X-ray data) is available free of charge at http://jbcs.sbq.org.br as PDF file.

Acknowledgments

This study was funded by the Coordenação de Aperfeiçoamento de Pessoal de Nível Superior - Brasil (CAPES) - Finance Code 001, by the National Council of Scientific and Technological Development - CNPq (process 305190/2017-2) and the Foundation of Support to Research and Innovation of Espírito Santo (FAPES PPE-Agro No. 76418880/16 and 76419363/16). We would also like to acknowledge LabPetro (UFES, Brazil) for performing FTIR and DSC measurements (Technical Cooperation Agreements No. 0050.0022844.06.4 and 5900.0112399.19.9), and FAPESP (process 2017/15850-0 and 2021/10066-5).

Author Contributions

Laura Patricia R. Figueroa was responsible for the organic synthesis work; Nayara A. dos Santos and Wanderson Romão for the MS analysis; Pedro Henrique O. Santiago and Javier Ellena for the X-ray analysis; Ana Camila Micheletti for the biological activity analysis; Valdemar Lacerda Junior and Warley S. Borges for the coordination of organic synthesis work and writing the article.

References

1. Shareef, M. A.; Sirisha, K.; Sayeed, I. B.; Khan, I.; Ganapathi, T.; Akbar, S.; Kumar, C. G.; Kamal, A.; Babu, B. N.; *Bioorg. Med. Chem. Lett.* **2019**, *29*, 126621. [Crossref]
2. El Malah, T.; Farag, H.; Hemdan, B. A.; Abdel Mageid, R. E.; Abdelrahman, M. T.; El-Manawaty, M. A.; Nour, H. F.; *J. Mol. Struct.* **2022**, *1250*, 131855. [Crossref]
3. Xu, Z.; *Eur. J. Med. Chem.* **2020**, *206*, 112686. [Crossref]

4. Gatadi, S.; Gour, J.; Shukla, M.; Kaul, G.; Das, S.; Dasgupta, A.; Malasala, S.; Borra, R. S.; Madhavi, Y. V.; Chopra, S.; Nanduri, S.; *Eur. J. Med. Chem.* **2018**, *157*, 1056. [Crossref]
5. Kumar, L.; Lal, K.; Kumar, A.; Paul, A. K.; Kumar, A.; *J. Mol. Struct.* **2021**, *1246*, 131154. [Crossref]
6. Pokhodylo, N.; Manko, N.; Finiuk, N.; Klyuchivska, O.; Matiychuk, V.; Obushak, M.; Stoika, R.; *J. Mol. Struct.* **2021**, *1246*, 131146. [Crossref]
7. Nural, Y.; Ozdemir, S.; Yalcin, M. S.; Demir, B.; Atabey, H.; Seferoglu, Z.; Ece, A.; *Bioorg. Med. Chem. Lett.* **2022**, *55*, 128453. [Crossref]
8. Tang, X.; Xie, M.; Sun, Y. X.; Liu, J. H.; Zhong, Z. C.; Wang, Y. L.; *Chin. Chem. Lett.* **2009**, *20*, 435. [Crossref]
9. Kraus, G. A.; Kumar, G.; Phillips, G.; Michalson, K.; Mangano, M.; *Bioorg. Med. Chem. Lett.* **2008**, *18*, 2329. [Crossref]
10. Majhi, S.; *Ultrason. Sonochem.* **2021**, *77*, 105665. [Crossref]
11. Li, L.; Chen, Z.; Zhang, X.; Jia, Y.; *Chem. Rev.* **2018**, *118*, 3752. [Crossref]
12. Mulzer, J.; *Nat. Prod. Rep.* **2014**, *31*, 595. [Crossref]
13. Freitas, L. B. O.; Ruela, F. A.; Pereira, G. R.; Alves, R. B.; de Freitas, R. P.; dos Santos, L. J.; *Quim. Nova* **2011**, *34*, 1791. [Crossref]
14. Alvarez, R.; Velázquez, S.; San-felix, A.; Aquaro, S.; de Clercq, E.; Perno, C.-F.; Karlsson, A.; Balzarini, J.; Camarasa, M. J.; *J. Med. Chem.* **1994**, *37*, 4185. [Crossref]
15. Buckle, D. R.; Rockell, C. J. M.; Smith, H.; Spicer, B. A.; *J. Med. Chem*. **1984**, *27*, 223. [Crossref]
16. Wang, X. L.; Wan, K.; Zhou, C. H.; *Eur. J. Med. Chem.* **2010**, *45*, 4631. [Crossref]
17. Genin, M. J.; Allwine, D. A.; Anderson, D. J.; Barbachyn, M. R.; Emmert, D. E.; Garmon, S. A.; Graber, D. R.; Grega, K. C.; Hester, J. B.; Hutchinson, D. K.; Morris, J.; Reischer, R. J.; Ford, C. W.; Zurenko, G. E.; Hamel, J. C.; Schaadt, R. D.; Stapert, D.; Yagi, B. H.; *J. Med. Chem.* **2000**, *43*, 953. [Crossref]
18. Melo, J. O. F.; Donnici, C. L.; Augusti, R.; Ferreira, V. F.; de Souza, M. C. B. V.; Ferreira, M. L. G.; Cunha, A. C.; *Quim. Nova* **2006**, *29*, 569. [Crossref]
19. Demmak, R. G.; Abdel-Mogib, M.; Bordage, S.; Samaillie, J.; Benssouici, C.; Bensegueni, A.; Neut, C.; Sahpaz, S.; *Fitoterapia* **2021**, *153*, 104987. [Crossref]
20. Wei, M. X.; Yu, J. Y.; Liu, X. X.; Li, X. Q.; Zhang, M. W.; Yang, P. W.; Yang, J. H.; *Eur. J. Med. Chem.* **2021**, *215*, 113295. [Crossref]
21. Liu, W.; Liu, C.; Liu, C.; Li, Y.; Pan, L.; Wang, J.; Jian, X.; *Chem. Eng. J.* **2021**, *424*, 130321. [Crossref]
22. Zhu, J.; Li, Z.; Lu, H.; Liu, S.; Ding, W.; Li, J.; Xiong, Y.; Li, C.; *Bioorg. Chem.* **2021**, *115*, 105232. [Crossref]
23. Tsai, C. Y.; Kapoor, M.; Huang, Y. P.; Lin, H. H.; Liang, Y. C.; Lin, Y. L.; Huang, S. C.; Liao, W. N.; Chen, J. K.; Huang, J. S.; Hsu, M. H.; *Molecules* **2016**, *21*, 145. [Crossref]
24. Adki, K. M.; Kulkarni, Y. A.; *Life Sci.* **2021**, *271*, 119202. [Crossref]
25. Hu, Y. S.; Han, X.; Yu, P. J.; Jiao, M. M.; Liu, X. H.; Shi, J. B.; *Bioorg. Chem.* **2020**, *98*, 103735. [Crossref]
26. Zhang, L.; Li, D.-c.; Liu, L.-f.; *Int. Immunopharmacol.* **2019**, *72*, 413. [Crossref]
27. Qin, D. D.; Yang, Z. Y.; Qi, G. F.; Li, T. R.; *Transition Met. Chem.* **2009**, *34*, 499. [Crossref]
28. Qin, D. D.; Yang, Z. Y.; Zhang, F. H.; Du, B.; Wang, P.; Li, T. R.; *Inorg. Chem. Commun.* **2010**, *13*, 727. [Crossref]
29. Jiang, Y.; Shi, X.; Xu, G.; Li, W.; *J. Chem. Res.* **2012**, *36*, 457. [Crossref]
30. Jiang, Y.; Ren, B.; Lv, X.; Zhang, W.; Li, W.; Xu, G.; *J. Chem. Res.* **2015**, *39*, 243. [Crossref]
31. Yang, T.; Shi, X.; Guo, L.; Gu, S.; Zhang, W.; Xu, G.; Li, W.; Jiang, Y.; *J. Chem. Res.* **2019**, *48*, 241. [Crossref]
32. Son, M.; Lee, H.; Jeon, C.; Kang, Y.; Park, C.; Lee, K. W.; Park, J. H.; *Bull. Korean Chem. Soc.* **2019**, *40*, 544. [Crossref]
33. Huang, L.; Zhang, B.; Yang, Y.; Gong, X.; Chen, Z.; Wang, Z.; Zhang, P.; Zhang, Q.; *Bioorg. Med. Chem. Lett.* **2016**, *26*, 5218. [Crossref]
34. Adki, K. M.; Kulkarni, Y. A.; *Life Sci.* **2020**, *250*, 117544. [Crossref]
35. Sheldrick, G. M.; *Acta Crystallogr., Sect. A: Found. Crystallogr.* **2015**, *71*, 3. [Crossref]
36. Sheldrick, G. M.; *Acta Crystallogr., Sect. C* **2015**, *71*, 3. [Crossref]
37. Dolomanov, O. V.; Bourhis, L. J.; Gildea, R. J.; Howard, J. A. K.; Puschmann, H.; *J. Appl. Crystallogr.* **2009**, *42*, 339. [Crossref]
38. Li, W.; Koike, K.; Asada, Y.; Yoshikawa, T.; Nikaido, T.; *J. Mol. Catal. B: Enzym.* **2005**, *35*, 117. [Crossref]
39. Silva, W. C. L.; Conti, R.; Almeida, L. C.; Morais, P. A. B.; Borges, K. B.; Júnior, V. L.; Costa-Lotufo, L. V.; Borges, W. S.; *Curr. Top. Med. Chem.* **2020**, *20*, 161. [Crossref]
40. Kuete, V.; *Planta Med.* **2010**, *76*, 1479. [Crossref]

Submitted: February 9, 2022
Published online: June 13, 2022